



UNIVERSITY OF LEEDS

This is a repository copy of *High contrast 3D proximity correction for electron-beam lithography: An enabling technique for the fabrication of suspended masks for complete device fabrication within an UHV environment*.

White Rose Research Online URL for this paper:
<http://eprints.whiterose.ac.uk/83485/>

Version: Accepted Version

Article:

Rosamond, MC, Batley, J, Burnell, G et al. (2 more authors) (2015) High contrast 3D proximity correction for electron-beam lithography: An enabling technique for the fabrication of suspended masks for complete device fabrication within an UHV environment. *Microelectronic Engineering*, 143. 5 - 10. ISSN 0167-9317

<https://doi.org/10.1016/j.mee.2015.01.020>

Reuse

Unless indicated otherwise, fulltext items are protected by copyright with all rights reserved. The copyright exception in section 29 of the Copyright, Designs and Patents Act 1988 allows the making of a single copy solely for the purpose of non-commercial research or private study within the limits of fair dealing. The publisher or other rights-holder may allow further reproduction and re-use of this version - refer to the White Rose Research Online record for this item. Where records identify the publisher as the copyright holder, users can verify any specific terms of use on the publisher's website.

Takedown

If you consider content in White Rose Research Online to be in breach of UK law, please notify us by emailing eprints@whiterose.ac.uk including the URL of the record and the reason for the withdrawal request.



eprints@whiterose.ac.uk
<https://eprints.whiterose.ac.uk/>

High contrast 3D proximity correction for electron-beam lithography: an enabling technique for the fabrication of suspended masks for complete device fabrication within an UHV environment

Mark C. Rosamond^a, Joseph T. Batley^b, Gavin Burnell^b, Bryan J. Hickey^b and Edmund H. Linfield^a

^aSchool of Electronic and Electrical Engineering, University of Leeds, Leeds LS2 9JT, UK

^bSchool of Physics & Astronomy, University of Leeds, Leeds LS2 9JT, UK

E-mail: m.c.rosamond@leeds.ac.uk

Abstract

Many devices, such as lateral spin valves, depend critically on the quality of interfaces formed between different materials, and hence require the entire device to be fabricated within an ultra-high vacuum environment. This is possible using angled deposition with a suspended mask such that, by depositing from specific angles, different patterns form on the substrate beneath. We use a bi-layer of MMA(8.5)MAA copolymer and PMMA patterned by electron-beam lithography (EBL) to form such a mask. It is necessary, though, to perform proximity effect correction (PEC) in EBL to achieve the correct spatial distribution of electrons, and hence produce the desired pattern in the developed resist. For bi-layer processes this is a three-dimensional (3D) correction since we must optimise for two different critical doses (one for the copolymer, the other for the PMMA) at defined 3D positions within the resist stack. We perform this 3D correction using the commercial software BEAMER produced by GenISys GmbH. We show that by applying manual shape segregation and modulation to the exposure pattern, prior to the “3D-PEC” algorithm, it is possible to achieve much higher contrasts in the spatial distribution of absorbed energy and hence significantly increase the processing window, and yield in the fabrication of suspended masks.

Keywords: E-beam lithography, suspended shadow mask, angled evaporation, 3D-PEC, GenISys BEAMER, lateral spin valve.

1. Introduction

The performance of many devices, for example lateral spin valves, depend critically on the quality of the interfaces formed between different materials [1, 2], and hence requires materials to be grown consecutively within an ultra-high vacuum (UHV) environment. However, to fabricate functional devices, it is often convenient to pattern one material before depositing the next. A commonly adopted approach is to combine a suspended mask structure with angled deposition such that, by changing the angle of deposition, shadowing by the mask forms different patterns on the underlying substrate (Figure 1). This technique is also used for devices requiring self-aligned structures since multiple layers can be patterned using the same lithographically defined feature.

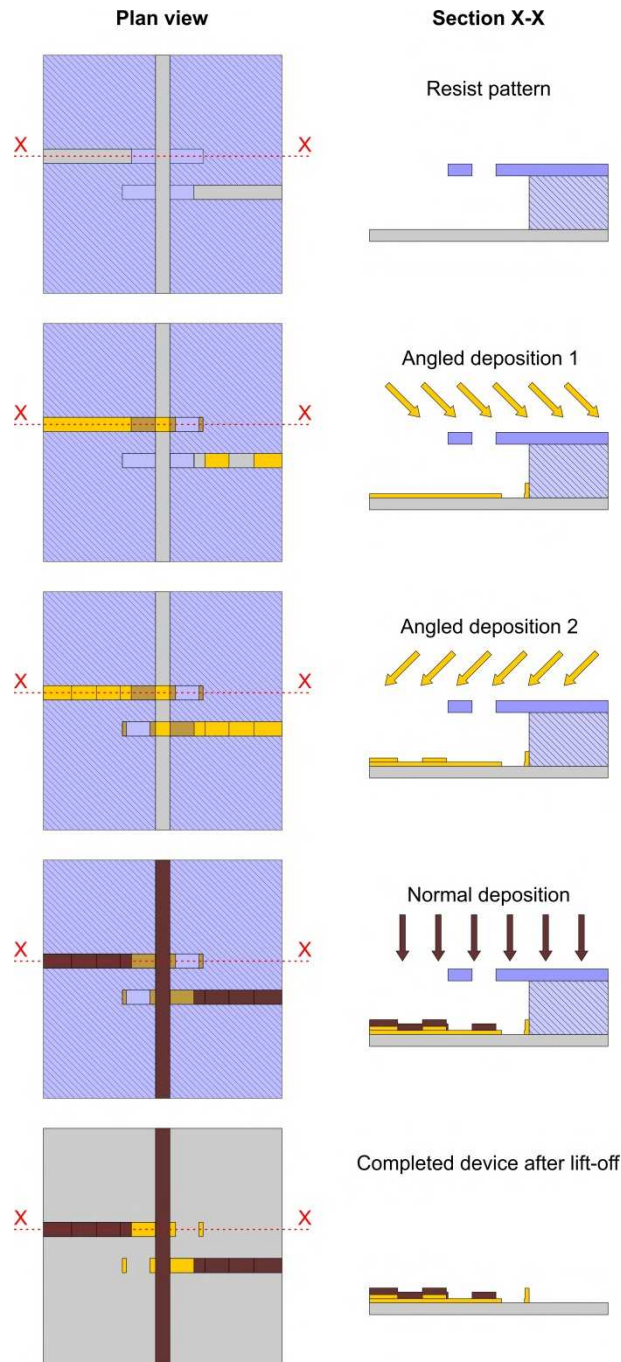


Figure 1: Schematic showing how different patterns form on a substrate by evaporating materials at specific angles through a suspended mask. Here, grey represents the substrate, hashed blue areas are copolymer and solid blue areas are PMMA. In the plan views, the PMMA has been treated as “transparent” such that the boundaries of the copolymer are visible. (For interpretation of the references to colour in this figure legend, the reader is referred to the web version of this article.)

The angled deposition technique has been applied to the fabrication of lateral spin valves [3], single-electron transistors [4], memristors [5] and Josephson junctions [6], amongst others. One of the earliest, and most widely implemented, suspended mask techniques uses a tri-layer system [7, 8]. Here, the top layer is an organic resist which is patterned via electron-, photon- or imprint- lithography. The middle layer forms the mask and is chosen to be chemically different from the organic materials used in the top “resist” and bottom “undercut” layers. Hence, is usually an inorganic material such as aluminium or germanium. The pattern, formed in the resist, is transferred via etching into this middle layer using a method that does not readily degrade the organic layers. For aluminium, a wet etchant, such as mixed phosphoric and nitric acid might be used whilst for germanium, an anisotropic dry etch using CF_4 can lead to more accurate pattern transfer. Finally, the bottom “undercut” layer is selectively removed from beneath the middle layer via isotropic wet or dry etching. Many different implementations of this method have been published including simplified versions requiring only bi-layer systems consisting of pairs of polymers; here, the top resist can be patterned, and the bottom polymer dissolved selectively – e.g. Polymethylglutarimide (PMGI) and PMMA [9].

A significant disadvantage of these approaches is that the degree of undercutting of the mask is equal for all parts of the pattern. Often, it is desirable to define large undercuts in some regions whilst maintaining minimal undercuts in others, since the structural integrity of the suspended mask can be compromised by having large undercuts where they are not required. To achieve this, it is necessary to be able to define the degree of undercutting lithographically. This is possible by utilising two resists possessing significantly different sensitivities and patterning them using electron-beam lithography (EBL). A “high dose” of electrons can be used to expose both resists, whilst a “low dose” can be used to make only the more sensitive resist soluble. If the more sensitive resist is the bottom film within the bi-layer, then the “low dose” can be used to define the regions where undercutting will occur. This method has been implemented previously in both simple bi-layer (MMA(8.5)MAA copolymer and PMMA) [10] – the resist structure we use – and tri-layer schemes (MMA(8.5)MAA copolymer, Ge, PMMA) [11].

In EBL, it is necessary to perform proximity effect correction (PEC) to exposure data in order to achieve the correct spatial distribution of electrons, and hence produce the desired pattern in the developed resist. This correction addresses scattering effects within the resist and substrate that spatially and energetically redistribute the electrons of the incident beam. A PEC algorithm modulates either the relative dose or the shape of an exposure pattern to account for these scattering effects.

In our work, the “high dose” value is determined by the critical dose of the (less sensitive) PMMA top layer while the “low dose” value is determined by the critical dose of the (more sensitive) copolymer bottom layer. The energy density absorbed in “low dose” regions must have an upper and lower bound since it is necessary to make the copolymer soluble whilst not significantly degrading the PMMA layer above. The proximity correction required for such exposure patterns is therefore a 3D problem since it must optimise for two separate doses, defined laterally and vertically, within the resist stack. The commercial software BEAMER (from GenISys GmbH [12]) incorporates a “3D-PEC” algorithm that can be used to solve such a problem.

The PEC algorithms implemented in BEAMER are based on the work of Pavkovich [13] where the energy density absorbed in the resist is modelled as the convolution between the exposure pattern and a point spread function. Furthermore, it is assumed that the developed resist boundary will follow a contour of critical absorbed energy, and hence a simple binary PEC problem can be reduced to considering only the energy density required at the edges of a given pattern. GenISys have modified this basic algorithm and extended its application to 3D-PEC problems [14]. The point spread function (PSF) used in a PEC algorithm is typically a description of the energy density absorbed in the resist as a function of distance from the beam. Such PSFs are usually estimated via Monte Carlo simulation techniques which reasonably

describe electron–matter interactions. Other effects such as lateral development, finite resist contrast and process blur can be incorporated into the PSF, however here we shall only consider electron scattering.

We will show that by manually performing shape modulation and segregation of “low dose” parts of the pattern prior to performing the 3D-PEC, it is possible to achieve much higher contrasts in the lateral distribution of absorbed energy and hence significantly increase the processing window and yield in the fabrication of suspended masks. Ultimately, this increase in dynamic range is due to the application of both shape and dose modulations.

2. Resist sensitivity and point spread functions

Suspended mask structures were formed in a resist bi-layer of MMA(8.5)MAA copolymer (500 nm) and PMMA 950k (200 nm) using 100 kV electron beam lithography with a JEOL JBX-6300FS system (exposure conditions: 100 kV, 500 pA beam current, 6 nm shot pitch). Methyl methacrylate–methacrylic acid copolymer, MMA(8.5)MAA EL11, and polymethylmethacrylate, PMMA 950k A5, were both purchased from Microchem Corp. Silicon wafers covered with a 100 nm thick oxide film were used as substrates. Figure 2(a) shows the experimentally measured contrast curves for 50% fill chequer board patterns written in single layers of PMMA and copolymer (each 400 nm thick) developed in 7:3 isopropanol–water for 90 s at 20 °C. The colouration overlaying the graph in figure 2(a) correspond directly to those shown in the table, figure 2(b), which describes the effects these doses have on the two resists.

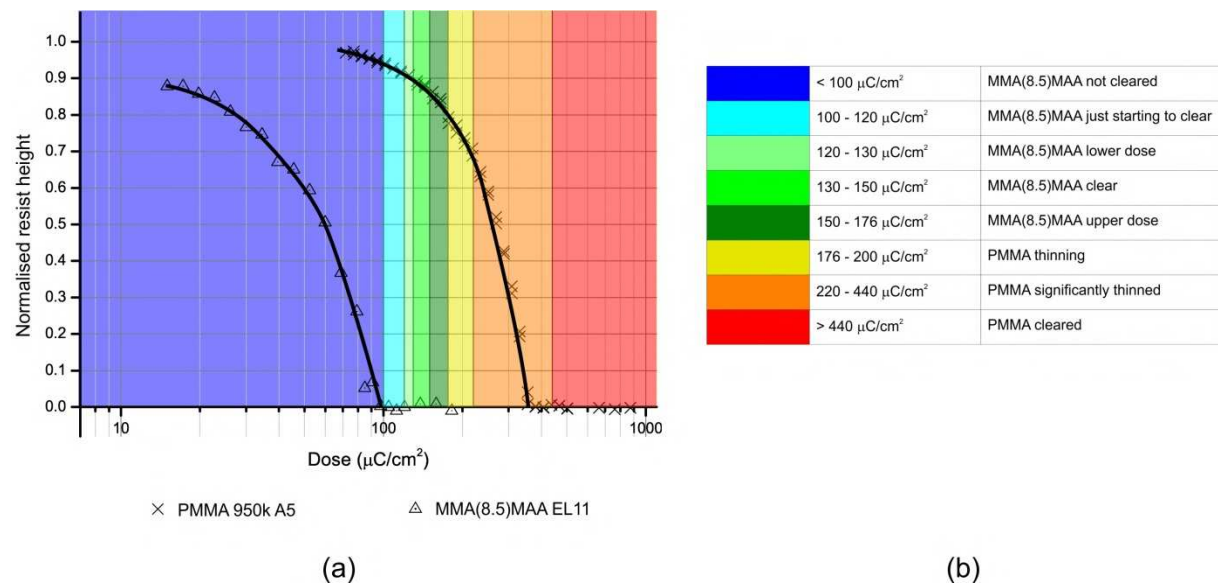


Figure 2(a): Contrast curves for PMMA and copolymer developed in 7:3 isopropanol–water. (b): Table correlating ranges of dose to resist behaviour.

As can be seen from figure 2, the “high dose” value (the exposure dose required to clear the PMMA) is 440 $\mu\text{C}/\text{cm}^2$ while the “low dose” value (the exposure dose required to clear the MMA(8.5)MAA but not significantly degrade the PMMA) should be between 120–176 $\mu\text{C}/\text{cm}^2$.

Point spread functions were simulated for a Si (700 μm) – SiO₂ (100 nm) – MMA(8.5)MAA (500 nm) – PMMA (200 nm) stack using the Monte Carlo simulator TRACER from GenISys GmbH [12]. A simulation of 10⁶ electrons at 100 kV was made and the resulting absorbed energy density within the resist recorded on a mesh consisting of 71 vertical elements and 301 radial elements. The grid spacing in the vertical direction was linear, whilst in the radial direction it was exponential. The incident electron beam was modelled as a Gaussian with a

radius of 0.75 nm and zero energy spread. Figure 3(a), the resulting 3D PSF, shows the simulated absorbed energy density within the resist ($\text{eV}/\mu\text{m}^2$) as a function of distance from the beam and depth within the resist stack (μm). From this, four, 2D PSFs were extracted from the vertical positions shown in figure 3(b), i.e. four data sets showing energy density as a function of radial distance. The PSF extracted from the centre of the PMMA layer (100 nm below the PMMA surface) was subsequently used by the “3D-PEC” algorithm in BEAMER as a model of electron scattering. This will be referred to as the “solution” PSF since it was used to calculate the proximity corrected exposure data. The other three PSFs extracted 50 nm below the surface of the PMMA, at the PMMA-copolymer interface and above the substrate (“top”, “interface” and “substrate” respectively), were used to check the quality of calculated exposure corrections.

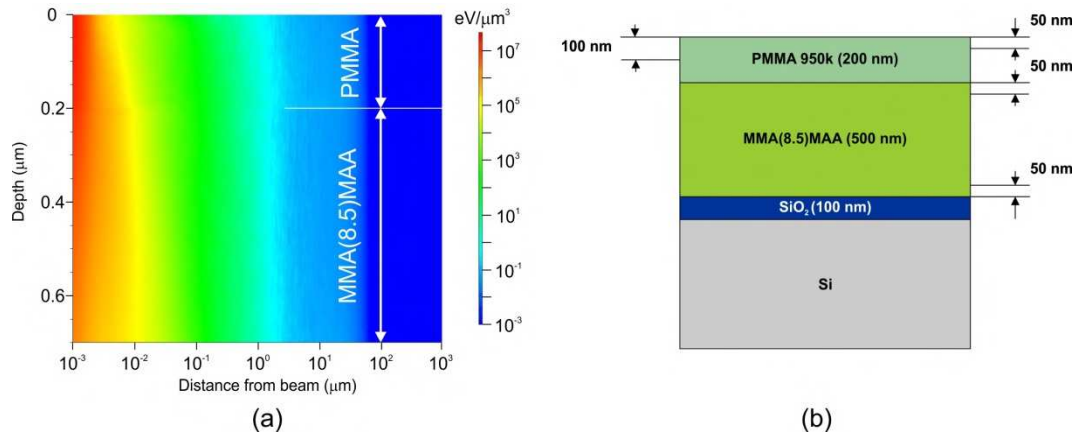


Figure 3(a): 3D point spread function showing the absorbed energy density in the resist stack as a function of depth and distance from the electron beam. (b): The simulated substrate and resist stack showing where 2D point spread functions were extracted.

BEAMER provides a function called “E-BEAM” which can be used to convolve exposure data files with 2D PSFs. Hence, at a defined vertical position in the resist, it is possible to simulate the absorbed energy density distribution which results from a given exposure pattern. The “E-BEAM” simulation returns energy densities in arbitrary units, however their effects on the resists can be estimated using the contrast curve data shown in figure 2. Therefore, these maps of simulated energy densities can reliably be used to compare the relative merits of different exposure corrections and, to a first approximation, estimate the form of the developed resist.

3. Direct application of the “3D-PEC” algorithm

Part of a typical design for a lateral spin valve is shown in figure 4(a) where the red regions are assigned a high, and the green regions a low, dose. This pattern was processed in BEAMER using the “3D-PEC” algorithm (3D-surface type defined by dose) with the “solution” PSF representing the electron scatter. Many different high-to-low dose ratios were tested within the “3D-PEC” in order to find a good exposure correction. Figure 4(b) and (c) show the simulated absorbed energy density maps resulting from two such corrected exposure data sets. Figure 4(b) shows the results for a high-to-low dose ratio of 1:0.155 whilst figure 4(c) shows the results for a ratio of 1:0.172.

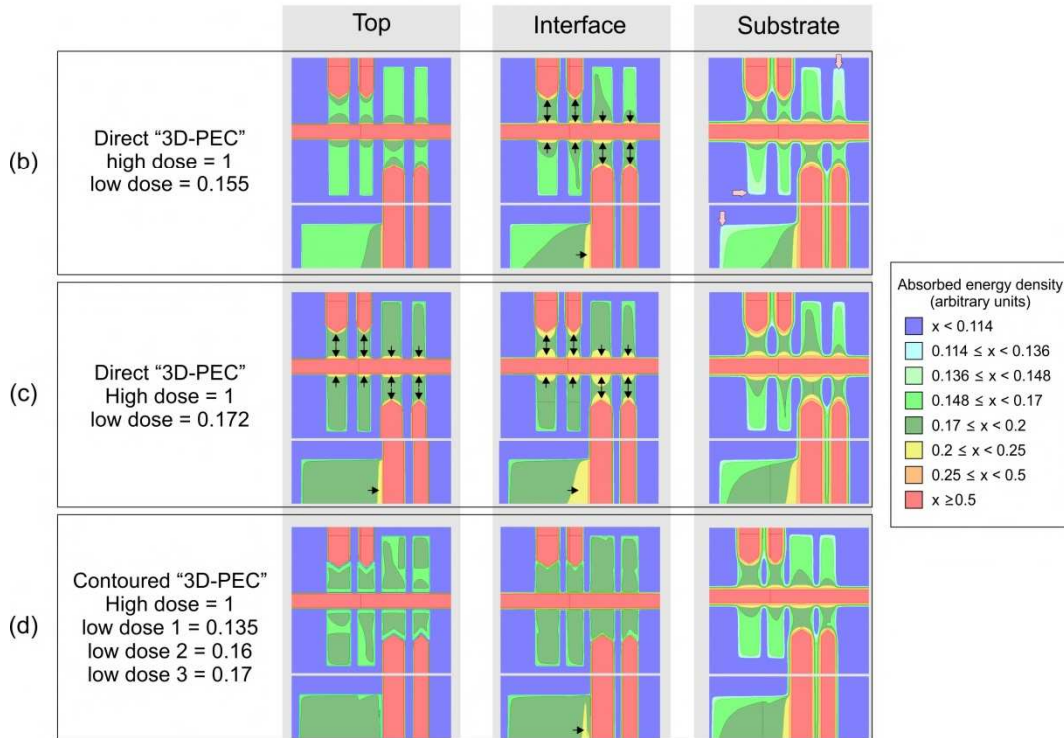
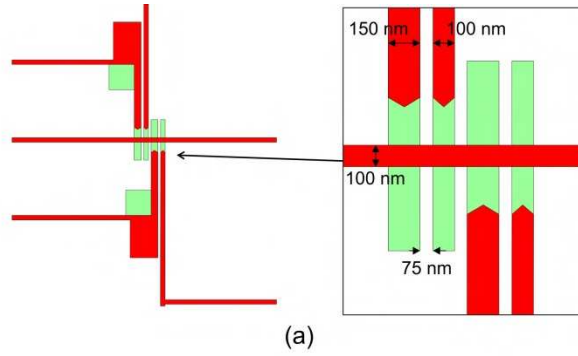


Figure 4(a): Part of a typical lateral spin valve design. Red areas are “high dose” and green areas are “low dose”.

Simulated absorbed energy density distributions within the resist resulting from exposing corrected data. (b): Pattern corrected using the “3D-PEC” algorithm with a high-to-low dose ratio 1:0.155 (c): Same as (b) but with a high-to-low ratio of 1:0.172. (d) Pattern corrected by the modified “contoured” processing. In pats (b), (c) and (d) black arrows indicate areas where the resist will be overexposed and pink arrows indicate areas of underexposure.(For interpretation of the references to colour in this figure legend, the reader is referred to the web version of this article.)

The colours used in figure 4(b-d) have been chosen to relate directly the simulated energy densities to the exposure doses show in figure 2. The implementation of the “E-BEAM” function is such that, by definition, an exposure dose of 1 arbitrary units, applied to a 50% fill pattern, results in an absorbed energy density of 0.5 arbitrary units following the pattern perimeter i.e. an exposure dose of 1 is the “dose-to-size” if an absorbed energy density of 0.5 represents the clearing energy density threshold of an infinite contrast resist. Therefore, in these simulations an absorbed energy of 0.5 arb. can be equated to a dose of 440 $\mu\text{C}/\text{cm}^2$ from the contrast curve in figure 2.

Referring to figure 4(b) it can be seen that the “3D-PEC” with a high-to-low dose ratio of 1:0.155 has produced an exposure correction that works well at the top of the resist, very slightly over exposes the PMMA layer at the PMMA-copolymer interface and slightly underexposes the copolymer at the resist-substrate interface. Degradation of the PMMA at the PMMA-copolymer interface is unacceptable because both

the bottom and top edges of the PMMA film define structures in an angled evaporation (see figure 1). Also, notice that the undercut regions are slightly undersized at the resist-substrate interface – this will result in significant material deposition on copolymer sidewalls which will, as a consequence, extend into the region intended to be undercut.

Figure 4(c) shows the results when the high-to-low dose ratio was increase to 1:0.172. This increase achieves the correct exposure of the copolymer at the resist-substrate interface at the expense of significant overexposure of the PMMA at both the PMMA-copolymer interface and the top of the PMMA.

In general, it is not possible, by correcting exposure data directly with the “3D-PEC” algorithm, to find a solution that is optimal for both the PMMA-copolymer and resist-substrate interfaces – the “3D-PEC” does not provide exposure data that generates an abrupt-enough contrast in energy density within the resist. Hence, exposure of these patterns results in a very narrow processing window (i.e. the copolymer at the substrate surface only just clears as the overhanging PMMA structures start to dissolve). We note that:

1. Low dose regions directly adjacent to high dose areas tend to be overexposed.
2. Low dose regions remote from high dose areas tend to be underexposed.
3. Low dose regions tend to be undersized at the resist-substrate interface.

We formed the hypothesis that one solution would be to expand the size of low dose regions, and then divide them into contours, defined by their proximity to high dose regions and assign different relative doses to them in the “3D-PEC” algorithm.

4. "Contoured" PEC processing

The modified processing had four critical stages: manual shape modulation of the low dose regions (positive size biasing followed by segregation into discrete regions determined by their distance from high dose regions); manual assignment of relative doses to these regions within the “3D-PEC” algorithm (3D-surface type defined by dose); solving the 3D-PEC based on the “solution” PSF, and finally, simulation of the absorbed energy density from the corrected exposure data, as a function of depth, within the resist. This process was iterated until an optimum solution was obtained.

For most exposure patterns similar to the one in figure 4(a) it was found the following parameters performed well. The "low dose" regions were positively biased by +15 nm. These regions were then divided into four separate patterns defined as "low dose" type regions bound by contours of 15, 40, 190 and more than 190 nm from "high dose" areas. 0–15 nm regions were defined as zero dose (removing them from the pattern). 15–40 nm regions were assigned a dose of 0.135 ("low 1"), 40–190 nm regions a dose of 0.160 ("low 2"), and regions greater than 190 nm a dose of 0.170 ("low 3"). High dose regions were then given a dose of 1 ("high") within the "3D-PEC" algorithm. These processing steps are shown in figure 5(a-d).

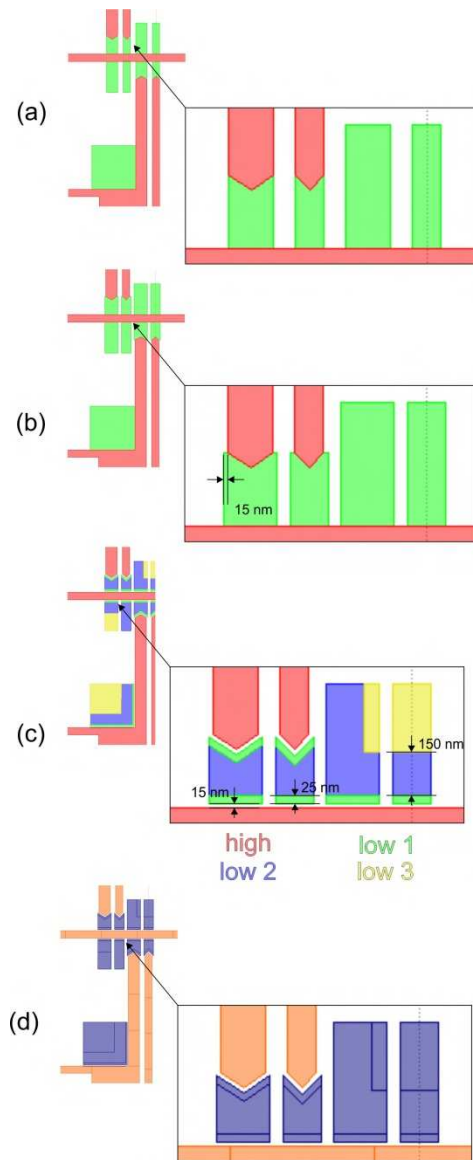


Figure 5. Contoured PEC processing. (a): Original pattern – red is "high dose" and green "low dose". (b): Biasing of "low dose" regions by +15 nm and removal of overlaps with "high dose" areas. (c): Segregation of "low dose" areas into different classes defined by contours described relative to "high dose" regions followed by removal of the "low dose" areas nearest the "high dose" regions. (d): The corrected exposure data - here, orange represent a dose of 1.8 arb. while blue represent doses ranging from 0.28 to 0.30 arb. (For interpretation of the references to colour in this figure legend, the reader is referred to the web version of this article.)

The simulated absorbed energy density maps for this correction are shown in figure 4(d). As can be seen the "contoured" processing gives, throughout the resist stack, a higher contrast in lateral energy density than was obtainable using the "3D-PEC" function directly – as is shown by comparison to figures 4(b) and (c). Only by using this "contoured" processing is it possible to generate sufficient energy densities in "low dose" areas at the resist-substrate interface, without overexposing the PMMA film significantly at the top or at its interface with the copolymer. The improvement is especially pronounced at the PMMA-copolymer interface where there is only one small region of overexposed PMMA in the "contoured" design. The energy density at the top of the resist stack is not uniform in "low dose" regions; however, for this application that is not an issue since the energy density is significantly below the clearing threshold of the PMMA.

5. Fabrication results

Using the "contoured" processing we have fabricated two and three layer lateral spin valves consisting of either permalloy ($\text{Ni}_{80}\text{Fe}_{20}$), copper or permalloy, copper and vanadium nano-wires. The materials were deposited using a bespoke evaporation system [15] with a base pressure 5×10^{-10} mbar and 3-axis sample rotation. Copper was deposited from an effusion cell whilst permalloy and vanadium were evaporated from a 4-pocket electron beam source. The sample was cooled during the deposition by a liquid nitrogen reservoir thermally connected to the sample mounting plate by a braided copper strap. This cooling is required to prevent the copolymer or PMMA reflowing or resist-fragments contaminating the deposited material.

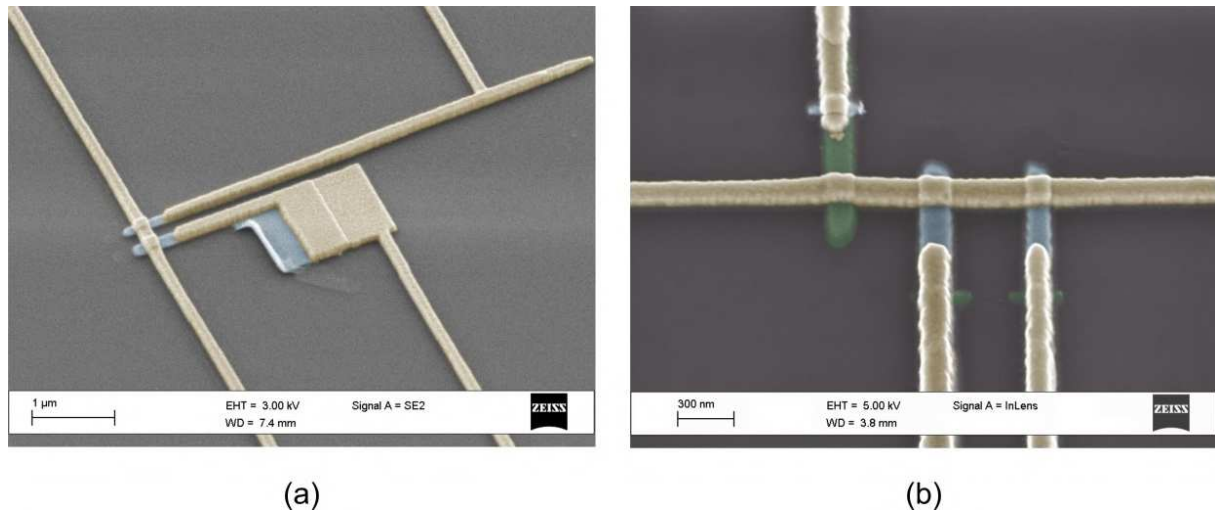


Figure 6 False coloured scanning electron microscope images of (a): Two layer lateral spin valve. (b): Three layer lateral spin valve.

Yellow areas are copper, blue areas are permalloy and green areas are vanadium. (For interpretation of the references to colour in this figure legend, the reader is referred to the web version of this article.)

Lateral spin valves were fabricated consisting of two ferromagnetic wires bridged by a nonmagnetic wire. Current driven through one ferromagnetic wire becomes spin polarized, due to differences in the conductivities for spin-up and spin-down electrons, which when injected into a nonmagnetic material induces a spin accumulation at the interface. This non-equilibrium spin density causes a diffusive spin current to flow along the nonmagnetic bridge. The spin current is detected as a non-local voltage at the neighbouring ferromagnetic – nonmagnetic interface. False coloured scanning electron microscope images of fabricated devices are shown in figure 6. These devices have been used to measure nonlocal spin and thermal transport properties [15].

6. Conclusions

We have shown that that BEAMER by GenISys GmbH provides a powerful and flexible tool for 3D proximity effect correction and absorbed energy density simulation. Exposure corrections are essential to form suspended mask structures in copolymer–PMMA resist bilayers, and we found that by applying manual pattern segregation and modulation to pattern data, prior to applying BEAMER's "3D-PEC" algorithm, it was possible to achieve much higher contrasts in the spatial distribution of absorbed energy than is possible using the "3D-PEC" alone. This increase in lateral energy density contrast significantly increased the processing window and yields of the suspended mask technique, and allowed the fabrication of complex lateral spin valve devices entirely within a UHV environment.

References

- [1] E. Villamor, M. Isasa, L. E. Hueso, and F. Casanova, *Phys. Rev. B*, 88, 184411 (2013), DOI: 10.1103/PhysRevB.88.184411.
- [2] P. Łączkowsk et. al., *App. Phys. Express*, 4, 063007 (2011), DOI: 10.1143/APEX.4.063007.
- [3] T. Yang, T. Kimura and Y. Otani, *Nature Phys.* 4, 851-854 (2008), DOI: 10.1038/nphys1095.
- [4] T. Weimann et. al., *Microelec. Eng.* 57-58, 915-918 (2001), DOI: 10.1016/S0167-9317(01)00456-7.
- [5] Q. Xia, J. J. Yang, W. Wu, X. Li, and R. S. Williams, *Nano Letters*, 10, 2909-2914 (2010), DOI: 10.1021/nl1017157.
- [6] Y. Takahide et. al., *Phys. Rev. Letters*, 85(9), 1974-1977 (2000), DOI: 10.1103/PhysRevLett.85.1974.
- [7] G. J. Dolan, *App. Phys. Letters*, 31, 337 (1977), DOI: 10.1063/1.89690.
- [8] J. Niemeyer, *PTB-Mitteilungen*, 84, 251–253 (1974).
- [9] B. Cord, C. Dames, K. K. Berggren and J. Aumentado, *J. Vac. Sci. Technol. B*, 24(6), 3139-3143 (2006), DOI: 10.1116/1.2375090.
- [10] F. Lecocq et. al., *Nanotech.* 22, 315302-315307 (2011), DOI: 10.1088/0957-4484/22/31/315302.
- [11] F. J. Jedema, Ph.D. thesis, University of Groningen, (2002).
- [12] www.genisys-gmbh.com
- [13] J. M. Pavkovich, *J. Vac. Sci. Technol. B*, 4(1), 159-163 (1986), DOI: 10.1116/1.583369.
- [14] N. Unal et. al., *Microelec. Eng.* 87, 940-942 (2010), DOI: 10.1016/j.mee.2009.12.002.
- [15] J. Batley et. al., *Institute of Physics Magnetism 2014*, 7-8 April, University of Manchester, UK (2014).

Acknowledgments

We gratefully acknowledge support from the UK Engineering and Physical Sciences Research Council.